Published in final edited form as:
Proteins. 2008 February 15; 70(3): 873–881. doi:10.1002/prot.21683.

Structural characterization of the zinc binding domain in cytosolic PSD-95 interactor (cypin): Role of zinc binding in guanine deamination and dendrite branching

José R. Fernández[1,2], **William J. Welsh**[3], and **Bonnie L. Firestein**[1,*]

[1]Department of Cell Biology and Neuroscience, Rutgers University, 604 Allison Road, Piscataway, New Jersey 08854-8082

[2]Molecular Biosciences Graduate Program, Rutgers University, 604 Allison Road, Piscataway, New Jersey 08854-8082

[3]Department of Pharmacology, University of Medicine and Dentistry of New Jersey (UMDNJ), Robert Wood Johnson Medical School and UMDNJ Informatics Institute, Piscataway, New Jersey 08854

Abstract

Dendrite morphology regulates how a postsynaptic neuron receives information from presynaptic neurons. The specific patterning of dendrite branches is promoted by extrinsic and intrinsic factors that trigger the activation of functional signaling pathways. However, most of the regulating factors and the biochemical mechanisms involved in regulating dendrite branching are unknown. Our laboratory previously reported that cypin (cytosolic PSD-95 interactor) plays an active role in regulating dendrite branching in hippocampal neurons. Cypin-promoted increases in dendrite number are dependent on guanine deaminase activity. In order to identify the specific structural role of zinc-binding in cypin-mediated dendrite branching and guanine deaminase activity, we employed computational homology modeling techniques to construct a three dimensional structural model of cypin. Analysis of the protein–ion sequestration scaffold of this model identified several histidines and aspartic acid residues responsible for zinc binding. Single substitution mutations in these specific sites completely disrupted the guanine deaminase enzymatic activity and rendered cypin unable to promote dendrite branching in rat hippocampal neurons. The specific zinc ion-binding function of each residue in the protein scaffold was also confirmed by Inductively Coupled Plasma–Optic Emission Spectrometry. Inspection of our structural model confirmed that His82 and His84 coordinate with the zinc ion, together with His240, His279, and Asp330, residues that until now were unknown to play a role in this regard. Furthermore, promotion of dendrite branching by cypin is zinc-dependent.

Keywords

molecular modeling; dendrite branching; zinc binding; ICP-OES; guanine deaminase

*Correspondence to: Bonnie L. Firestein, Department of Cell Biology and Neuroscience, Rutgers, the State University of New Jersey, Nelson Biological Laboratories, 604 Allison Road, Piscataway, NJ 08854-8082. E-mail: E-mail: firestein@biology.rutgers.edu.

INTRODUCTION

Regulated neurite outgrowth in developing neurons determines how incoming electrical and/or chemical signals are processed. A change in the dendritic branching pattern of a neuron can alter the neuron's ability to communicate with other neurons, changing signaling networks. Thus, elucidation of intracellular mechanisms that regulate dendritic growth and arborization in growing neurons is important for understanding normal neuronal development as well as disorders that result from aberrant dendritic growth.[1] Several intrinsic molecules in neurons have been shown to regulate dendrite branching, including cytosolic PSD-95 interactor (cypin).[2–4] Cypin was previously cloned as a guanine deaminase that is highly expressed in the human and rodent brain.[2,5,6] Cypin is also member of the metal-dependent amino-hydrolase family, which shares a nine-residue motif, PG[L]VDTHIH, which is thought to be responsible for zinc ion binding.[5] Despite the central role played by cypin in neuronal development, many unanswered questions remain pertaining its three-dimensional structure, the actual amino acids that coordinate zinc ion binding to cypin, whether cypin does in fact bind zinc, and the effect of zinc binding on dendrite branching.

To address the location of the zinc ion within the context of cypin's three dimensional structure, we constructed a structural model of the rat ortholog of cypin. Evaluation of our cypin model for zinc ion binding contrasts with the previous prediction that there is solely a nine amino acid domain, which contains two crucial histidine residues involved in zinc ion binding.[5] We have identified two novel histidines and one aspartic acid residue, which are also part of the zinc ion coordination. This novel binding scaffold of cypin exhibits significant differences with the available guanine deaminase protein structure from *Bacillus subtilis*, in which the zinc ion in this structure is coordinated by two cysteines, one histidine, and a water molecule.[7,8]

To evaluate the validity of our cypin structural model, we show that single alanine substitution mutations of the predicted residues lack wild type guanine deaminase activity. Furthermore, overexpression of these cypin protein mutants in cultured hippocampal neurons fails to increase primary and secondary dendrites. Authentication of specific binding of zinc to cypin was verified using Inductively Coupled Plasma-Optical Emission Spectrometry (ICP-OES), and our results confirm that our structural model correctly predicts those amino acids that are involved in zinc binding to mammalian cypin. In addition, our data suggest that zinc binding to cypin is essential for guanine deaminase activity and that this ion–protein biointerface may modulate the required global three-dimensional conformation of the protein to interact with other intrinsic molecules that aid in cypin-promoted dendrite branching in hippocampal neurons.

MATERIALS AND METHODS

Homology modeling

The crystal structure of the guanine deaminase from *C. acetobutylicum* with bound guanine in the active site (PDB ID = 2I9U)[9] was chosen as the template for the homology modeling of rat cypin with NCBI Accesion No. NP_113964. The primary cypin sequence was submitted to the Swiss-Modeller homology modeling tool [http://swissmodel.expasy.org//SWISS-MODEL.html], and the resulting structure was submitted to the WHATIF server for structural verification (http://www.cmbi.kun.nl/gv/servers/WIWWWI/).[10] The initial homology model was also constructed using the InsightII 2000 software package [http://www.accelrys.com; Insight©, 2000]. 2I9U and rat cypin structurally conserved regions (SCRs) were assessed by secondary structure predictions using three different programs: nnpredict,[11] PHD,[12] and JPRED,[13] and were identified based on sequence and functional similarity. The three dimensional coordinates within SCRs were copied from the template of 2I9U to cypin. De novo loop generation was

employed to yield the coordinates for variable regions (VRs), which consisted of loop regions not contained within the SCRs. In the existing 2I9U structure, an iron cation (Fe^{3+}), a glycerol, and a guanine molecule are present in the structure, but only the cation has been observed to aid in the coordination between guanine and binding site residues. Previous initial work using purified recombinant guanine deaminases was found to contain an atom of zinc per protein monomer. [5] Therefore, the Fe^{3+} ion was manually extracted from the template structure and replaced with a Zn^{2+} ion positioned into the preliminary cypin model. After subsequent resolution of atomic clashes, the protein complex was submitted to Energy Minimization (EM) to refine the cypin structural model.

Energy minimization

Refinement of the cypin structural model was conducted by EM using AMBER 9.0 force field[14] in a vacuum. The system was energy-minimized in two phases: first, 200 iterations of constrained steepest descent (SD); second, 300 iterations of conjugated gradient (CG) minimization was conducted on the entire system.

Site-directed mutagenesis

The cypin zinc-binding alanine substitution mutants were prepared using the QuickChange II site-directed mutagenesis kit (Stratagene). All the substitution mutations were performed using the pEGFP-C1 and pGEX4-T1 vectors containing the *Rattus norvegicus* wild type full length sequence of cypin, using a cloned *Pfu* polymerase and *Dpn*I endonuclease from Stratagene (La Jolla, CA). The following forward primers were used: H71A, 5′-GAT CAG AGA GCT GAG CCA CGC TGA GTT CTT CAT GCC AG-3′; H82A, 5′-GGC CTT GTT GAT ACA GCC ATC CAT GCC CCT CAG TAT GCC-3′; I83A, 5′-GCC TTG TTG ATA CAC ACG CCC ATG CCC CTC AGT ATG CC-3′; H84A, 5′-CTT GTT GAT ACA CAC ATC GCT GCC CCT CAG TAT GCC-3′; H240A, 5′-GTA CAT CCA GAG CGC TAT AAG TGA AAA TCG TG-3′; H279A, 5′-CAA ACA AAA CAG TGA TGG CTG CTG GCT GCT ACC TTT CTG-3′; D330A, 5′-GAT AGG GCT TGG GAC AGC TGT GGC TGG TGG TTA C-3′. For the generation of individual mutants, the following were mixed in a PCR-tube and placed in a thermal cycler: 10 ng plasmid containing a *Rattus norvegicus* wild type sequence of cypin, 5 ng of each forward and reverse primers, 10× *Pfu* polymerase buffer, dNTPs, sterile distilled H_2O and *Pfu* DNA polymerase to a volume of 50 μL. The following thermal cycle protocol was followed: (1) denaturing temperature 95°C, 30 s, cycled once, (2) denaturing temperature 95°C, 30°s, (3) annealing temperature 55°C, 60°s, (4) extension temperature 68°C, 530°s (1 min per kb), and (5) Steps 2–4 were cycled 16 times. Then, *Dpn*I restriction enzyme (10 U) was added when the protocol was complete, and incubated at 37°C for 1 h to completely digest the methylated (wild type template) plasmid. Finally, the cypin zinc-binding mutant sequences carrying the desired mutations were transformed into *E. coli* DH5α supercompetent cells, and plasmid DNA from selected clones was isolated and confirmed by sequencing.

Antibodies

Mouse anti-MAP2 was purchased from Sigma–Aldrich, and Cy2- and Cy3-conjugated secondary antibodies were purchased from Jackson Immuno Research Laboratories (West Grove, PA). Rat anti-GFP was a gift from Dr. Shu-Chan Hsu (Rutgers University, Piscataway, NJ).

Guanine deaminase assay

To measure guanine deaminase enzyme activity, COS-7 cells were transfected with the indicated plasmids using Lipofectamine 2000 (Invitrogen) and 2.5 μg of DNA per 100 mm culture dish of pEGFP-C1 vector alone, containing the *Rattus norvegicus* wild type full length or mutant sequences of cypin. After 48 h of expression, cells were washed twice with

phosphate-buffered saline (PBS) and scraped into GDA lysis buffer (150 m*M* NaCl, 25 m*M* Tris-HCl, pH 7.4 and 1 m*M* PMSF). Lysates were homogenized by passing them through a 25-gauge needle five times and centrifuged at 10,000 rpm at 4°C for 10 min. Concentration of cytosolic proteins in the supernatant was measured using the Bradford Assay. Protein samples were resolved by SDS-PAGE for equal cypin expression verification (data not shown). Fifty micrograms of lysate was then used for each guanine deaminase sample assay in GDA lysis buffer containing 0.025 U/mL xanthine oxidase (Sigma–Aldrich), 0.002 U/mL peroxidase (Sigma–Aldrich), Amplex Red reagent (Molecular Probes, Eugene, OR), and 125 m*M* guanine (Sigma–Aldrich, St. Louis, MO). Negative controls were performed using protein lysates in assay solution with no guanine added. Negative control and samples were incubated at 37°C, and absorbance at 512 nm using a single beam Genesys 10 UV/Vis Spectrophotometer (Spectronic, Garforth, UK) was measured during the indicated time intervals after samples were centrifuged at 10,000 rpm for 1 min to remove insoluble guanine. Experiments were performed in triplicate and results were normalized by subtracting nonspecific background absorbance from the negative controls.

Neuronal culture, transfection, and dendrite branching number analysis

Neuronal cultures were prepared from hippocampi of rat embryos at 18 days of gestation as previously described.[2–4] After 10 days *in vitro* (d.i.v.), neurons were transfected using the Effectene reagent (QIAGEN, Valencia, CA) as is done routinely in our laboratory.[3,4,15] Cultures were allowed to express the transfected proteins for 48 h. Images of transfected hippocampal neurons were taken as described previously,[4] and neurons were confirmed by MAP2 immunostaining. Primary and secondary dendrites were counted as previously described.[3,4,15] To acquire unbiased dendrite number counts, the analyzing person was blinded to the transfection condition.

Immunohistochemistry

Hippocampal neurons were plated on coverslips and were fixed and blocked as previously described.[4] Rat anti-GFP and mouse anti-MAP2 antibodies (both at 1:1000 dilutions) were added at room temperature for 2 h. Coverslips were washed with PBS and incubated at room temperature with Cy2-conjugated donkey anti-rabbit IgG and Cy3-conjugated donkey anti-mouse IgG secondary antibodies (1:250 dilutions).[4] Coverslips were mounted onto frosted glass microscope slides using Fluormount G (Southern Biotechnology). Labeled cells were visualized by immunofluorescence using an Olympus IX50 microscope with a Cooke Sensicam charge-coupled device cooled camera, fluorescence, imaging system, and Image Pro software.

Protein purification

GST, GST-cypin (wild-type), and GST-cypin mutants were expressed in *Escherichia coli* cultures grown in Luria-Bertani (LB) media and purified using glutathione-Sepharose beads (Amersham Biosciences, Piscataway, NJ). Transformed cells were grown overnight and seeded in a 100 mL LB media culture at 37°C until reaching an OD_{600} of 0.8. To obtain GST fusion protein products that have lower solubility, we induced cells with a low IPTG concentration (1 m*M*) and then grown overnight at room temperature. After centrifugation, cell pellets were homogenized in 10 volumes of ice-cold MTBSE buffer (1× PBS + 2 m*M* EDTA) containing 1 m*M* phenylmethylsulfonyl fluoride (PMSF) and sonicated two times for 20 s each. Triton X-100 was added to 1%, and proteins were extracted for 1 h at 4°C. Extract/beads were then loaded into the appropriately sized columns and were washed with 100 column volumes of MTBSE buffer, 1% Triton X-100, and 1 m*M* PMSF. Proteins were eluted consecutively with five column volumes of MTBSE containing 1% Triton X-100 and 2.5 mL of elution buffer (1× PBS + 1% SDS + 100 m*M* NaCl + 20 m*M* glutathione, pH 8.0). Finally, eluates were dialyzed extensively against PBS to remove glutathione and salt excess.

Zinc binding assay

GST fusion proteins were purified from *E. coli* as stated above using glutathione sepharose and eluted from the beads with excess glutathione. The zinc that was incorporated into cypin was from the yeast extract in the LB medium taken up by the bacteria culture. Eluates were dialyzed extensively against PBS to remove the glutathione. Equal concentrations of protein samples (determined by Bradford protein assay and confirmed by SDS-PAGE) were subjected to Inductively Coupled Plasma-Optical Emission Spectrometry (ICP-OES) using a Varian Vista-PRO Model CCD Simultaneous ICP-OES spectrometer (VISTA, Palo Alto, CA), and the absorbance intensity at 213 nm (specific for incinerated zinc) was compared with a standard curve of known $ZnCl_2$ concentrations (10 μ*M*, 100 μ*M*, 1 m*M*, 5 m*M*, and 10 m*M* in elution buffer) to calibrate the instrument. Radiation intensities were measured at 213 nm, and the intensity ratios of samples to GST were plotted.

Statistical analysis

Dendrite counts were performed using $n \geq 35$ per condition, and statistical significance was determined by ANOVA followed by a Dunnett multiple comparisons test using $P < 0.05$ as a significant difference. For the zinc-binding assay, protein samples were assayed in triplicate. For ICP-OES measurements, samples were compared using ANOVA followed by the Student–Neuman–Keuls comparison test also using $P < 0.05$ as a significant difference.

RESULTS

Structure of cypin by homology modeling

The lack of an available three dimensional structure of cypin, a guanine deaminase that has been shown to regulate dendrite patterning in neuronal development,[3] motivated us to develop an *in silico* model of the protein structure using homology modeling. The determination of a structural model facilitates the bunderstanding of mechanisms that may contribute to the enzymatic activity of this protein. We identified the metal-dependent guanine deaminase from *C. acetobutylicum* with bound guanine in the active site [PDB ID = 2I9U] as the most suitable structural template for cypin, both being members of the metal-dependent hydrolases with a 56% of primary sequence similarity. The multiple sequence alignments of guanine deaminase between human, rat and *C. acetobutylicum* as template are shown in Figure 1 and were conducted using the ClustalW1.8 routine with a Protein Gap Open penalty of 10.0, Gap Extension penalty of 0.2, END GAP of −1, GAP DIST of 4 with the Gonnet Matrix.[16] This template contains conserved functional secondary structural motifs as verified by secondary structure predictions. Secondary structure prediction of the rat cypin (guanine deaminase) using three methods was performed, and the consensus α-helix and β-strand structures in the primary sequence of the protein are shown in Figure 2(A). A WHATIF check of the 1P1M template structure was performed prior to the model assembly, adjusting for slight structural modifications. To identify structurally and functionally conserved regions across the family of the metal-dependent hydrolases, multiple sequence alignment was performed between these sequences and the sequence of rat cypin. The multiple alignments were followed by a pairwise sequence alignment between cypin and the template 2I9U and, as expected, functionally conserved motifs were found, allowing us to determine a three dimensional homology model of cypin as shown in Figure 2(B).

Identification of novel amino acid residues involved in zinc ion binding to cypin

To determine the specific zinc-binding residues of the rat cypin protein structure, the Fe^{3+} ion was manually extracted from the guanine deaminase template structure and replaced with a Zn^{2+} ion positioned into the preliminary cypin model. Further de novo loop generations along with energy minimization were assessed to confirm zinc metal ion stabilization. It was

previously reported that histidines 82 and 84 (His82, His84) are involved in zinc binding to cypin[5]; however, our model also reveals for the first time that His240, His279, and Asp330 are likely to be coordinating residues by virtue of the orientation of their side chains and their close proximity (υ.0 Å) to the zinc ion. The specific residues His82 and His84, previously predicted to bind zinc by Snyder and coworkers,[5] and His279 and Asp330 were identified within a close intramolecular distance. A specific tetra-coordinate system was observed to be consistent with metal ion stabilization as shown in Figure 3 with an additional amino acid, His240, in high proximity, indicating a possible folding stabilization of the zinc domain scaffold. The novel zinc ion binding motif in cypin differs when compared with the only available structure of a guanine deaminase protein from *Bacillus subtilis*,[7,8] which has two cysteines, one histidine, and a water molecule as its zinc binding coordination.

Guanine deaminase activity is absent in zinc binding residues mutants

The binding of zinc to cypin is thought to play an essential role in mediating cypin's guanine deaminase activity.[3,5] To confirm our cypin structural homology model, and specifically the zinc binding scaffold, we mutated the specific residues found to be responsible for the coordination of the zinc ion in the protein structural model and other residues as control. Using site-directed mutagenesis, we created single alanine substitutions for each residue (His82, His84, His240, His279, and Asp330) using constructs that encode amino terminally GFP-tagged mutants. His71 and I83 were also mutated to ala-nines to serve as negative controls for eliminating zinc binding and to assure that lack of zinc binding to other mutants is not solely due to a disruption in the overall three dimensional structure of cypin. COS-7 cells overexpressing wild type or mutant cypin proteins were lysed, and the lysates were subjected to a colorimetric guanine deaminase activity assay. Single substitution mutations of the predicted residues that bind to the zinc ion caused a drastic attenuation of wild type guanine deaminase activity measured over time (Fig. 4). As expected, mutation of His71 and I83 had no effect on cypin's guanine deaminase activity, suggesting that these mutants are not disturbing the required three dimensional structure of the protein, and therefore the wild type enzymatic activity remain unaffected (Fig. 4). These results indicate that the lack of wild type deaminase activity in the zinc binding mutants is specific to those amino acids predicted to bind zinc. These data indicate that His82, His84, His240, His279, and Asp330, which are predicted to be essential for zinc binding, are also necessary for cypin's enzymatic activity.[3,5]

Zinc binding residue mutations eliminate cypin-promoted increases in dendrite branching

Given that cypin has been shown to increase dendrite branching when overexpressed in primary cultures of hippocampal neurons and that the guanine deaminase activity is necessary for this increase in dendrites,[3] we tested whether mutating amino acids that bind zinc affects cypin-promoted increases in primary and secondary dendrite number. We transfected embryonic rat hippocampal neurons at 10 d.i.v. with the same cDNAs encoding cypin-GFP constructs that we used in the guanine deaminase assay (Fig. 3) and assessed primary and secondary dendrite number. As expected, overexpression of wild type cypin resulted in a significant increase in both primary and secondary dendrites when measured at 12 d.i.v. [Fig. 5(A–C)] when compared to GFP expressing neurons. Cells overexpressing the single alanine substitution mutants of cypin that are predicted to lack zinc binding also lack the ability to increase both primary and secondary dendrites when compared to control GFP expressing neurons [Fig. 5 (A–C)]. In contrast, when residues that are predicted not to be involved in zinc binding (His71 or Ile83) are mutated, cypin's ability to increase dendrite number above control (GFP) conditions is not eliminated [Fig. 5(A–C)]. It does appear, however, that there is a small attenuation in the number of cypin-promoted dendrites, possibly due to reasons not related to zinc binding [Fig. 5(B)]. These data suggest that the predicted structural zinc binding amino acids are necessary for promoting neuronal dendrite branching.

Inductively coupled plasma-optical emission spectrometry demonstrates that His82, His84, His240, His279, and Asp330 are essential residues for zinc binding to cypin

To quantitatively demonstrate whether the predicted amino acids in our homology structure model of cypin are essential for zinc binding, we measured the amount of zinc bound to purified GST-cypin fusion proteins expressed from transformed bacteria. Equal concentrations of GST-cypin or GST-cypin mutants [Fig. 6(A)] were subjected to Inductively Coupled Plasma-Optical Emission Spectrometry (ICP-OES), and the radiation emission intensity at 213 nm was measured and compared to the control GST protein. We found that the levels of zinc ions bound to the single alanine mutants were significantly less than the level of zinc bound to wild type cypin [Fig. 6(B)], indicating that our predicted zinc binding residues indeed help to stabilize zinc binding in the secondary and tertiary structures of cypin. Mutation of His71 or Ile83 had no effect on zinc binding, as expected [Fig. 6(B)].

DISCUSSION

In this study, we used homology modeling to predict the three-dimensional structure of the multifunctional protein cypin. Although the *B. subtilis* guanine deaminase protein structure is available (pdb ID: 1WKQ; 7), the mammalian cypin proteins do not share any sequence similarity even though they share the same cellular substrate and enzymatic function. The rat, human, and mouse guanine deaminase orthologues contain 454 amino acids with a nine-residue metal-binding motif and a four-residue PDZ binding motif at the C-terminus, which is responsible for PSD-95 interaction at the postsynaptic density in neurons.[2] On the other hand, the *C. acetobutylicum* guanine deaminase structure contains 428 residues, which align with the mammalian orthologue sequences. This guanine deaminase protein also contains the putative nine-residue metal binding motif, and the predicted residues that bind to zinc in the rat and human guanine deaminase sequence are conserved (Fig. 1).

Cypin has been shown to be involved in purine metabolism by catalyzing the break-down of guanine to xanthine and ammonia.[5] In addition, cypin has been reported to act as a regulator of PSD-95 clustering in neurons[2] and as an important cellular intrinsic factor that regulates dendrite branching in hippocampal neurons.[3,4] How these three functions of cypin are related has been a focus of study for our laboratory.

The primary finding of our current work is that in addition to two previously known amino acids, we have identified three novel amino acids that play an important role in zinc binding to cypin. Furthermore, we have now definitively shown that zinc binding to cypin regulates guanine deaminase activity, which has been hypothesized but never demonstrated. Our current mutational analysis suggests that single substitutions of histidines 82, 84, 240, and 279 and aspartate 330 to alanine, a small nonpolar side-chain that does not allow for coordination to zinc, lowers the affinity of cypin for Zn^{2+}. This result suggests that our predicted residues play an important role in the stabilization of the native fold of cypin and ensure optimal residue orientation of key residues (His82, 84, 240, 279 and Asp330) within the binding site. Furthermore, cypin variants, which contain mutations in the zinc binding region, lack the ability to increase both primary and secondary dendrites in rat hippocampal neurons when compared to control neurons. These same residues also disrupt the guanine deaminase activity of the wild type protein, suggesting that the predicted zinc binding scaffold is necessary for both activities and that a functionally active enzyme is crucial for dendrite formation. This is consistent with previous work using deletion mutations of a nine-residue motif (amino acids 76–84) in cypin, resulting in attenuation of guanine deaminase activity and cypin-promoted increases in dendrite number. [3] However, since disruption in cypin protein folding due to this large deletion could possibly disrupt the overall three dimensional structure of cypin, our mutation of single amino acid residues offers stronger evidence supporting a role for zinc binding, and hence guanine deaminase activity and in dendrite formation.

What are the sources of zinc that can influence cypin's guanine deaminase activity? In our cell-free zinc-binding assay, the source of zinc that was incorporated into the proteins during bacterial culture growth was obtained from yeast extract used in the LB media (0.2 m*M*[18]). This is a much higher concentration of that found in the media used to grow COS-7 cells for guanine deaminase assays (5 μ*M* from the fetal bovine serum[19,20]). It is unknown the concentration range of cellular zinc that is needed for cypin's effect on dendrite branching. But interestingly, it was previously reported that zinc is released from the perinuclear area, including the endoplasmic reticulum, in mast cells in response to stimulation and can act as a second messenger[21]; however, it is unknown whether this occurs in neurons and whether this pool of zinc can activate cypin and promote dendrite branching.

Since the global three-dimensional structure of a protein determines the accessible motifs and residues necessary for its enzymatic activity, the lack of available solved structures for cypin and/or related proteins has hampered our understanding of specific mechanisms of protein action leading to cellular processes, such as purine metabolism and neuronal development. In the absence of a high-resolution crystal structure, rational predictions of protein structure using bioinformatics tools can provide valuable insight into protein structure–function relationships when combined with experimental validation. Using the guanine deaminase from *C. acetobutylicum* as template to predict cypin structure by homology, we determined that the mammalian guanine deaminase contains a TIM barrel tertiary structure and a novel zinc ion-binding domain. Analysis of the *Bacillus subtilis* guanine deaminase crystal structure[7,8] suggests that the residue–ion binding components diverge, where this bacterial enzyme contains a cysteine–histidine coordination to bind zinc and the mammalian guanine deaminase/cypin utilizes four histidines (at positions 82, 84, 240, 279) and an aspartate (at position 330) to bind zinc. A high percentage of zinc-containing protein crystal structures contain at least three histidines involved in zinc binding, suggesting that our predicted interaction is an ion–protein interface by analysis using the Metalloprotein Database. [16]

The validation of the specific binding of zinc to cypin was established using ICP-OES, and our results confirmed that the protein structural model positively contains the zinc binding scaffold interface of the mammalian guanine deaminase protein. Our data suggest that the zinc binding stability of cypin is crucial for the guanine deaminase activity, possibly participating in the deamination reaction mechanism. This ion–protein bio-interface may alter the overall three-dimensional conformation of cypin, thus possibly regulating its interaction with additional intrinsic molecules that may facilitate or promote dendrite branching. For example, cypin binds tubulin heterodimers and promotes microtubule polymerization, leading to increased dendrite number in growing hippocampal neurons.[3] As of yet, there are few available templates for modeling the interaction between cypin and tubulin. Interestingly, the collapsin response mediator protein (CRMP) homology domain of cypin mediates this interaction, and a crystal structure for CRMP has just been published.[22] Furthermore, CRMP also binds zinc, and it too uses a three histidine motif.[22] Thus, our ongoing studies are focused on identifying critical residues for cypin's interaction with tubulin and, together with our current study, will aid in our understanding of cypin's structure and function in neurons.

Abbreviations

CRMP, collapsin response mediator protein homology; Cypin, cytosolic PSD-95 interactor; GDA, guanine deaminase assay; GFP, green fluorescent protein; GST, glutathione sepharose transferase; ICP-OES, inductively coupled plasma-optic emission spectrometry; PDB ID, protein data bank identification code; PSD-95, postsynaptic density-95.

ACKNOWLEDGMENTS

We want to thank Yuval Eisenberg for constructing the GFP-Cypin H240A plasmid and Vladyslav Kholodovych, Ni Ai, and Paul Field for their technical support.

Grant sponsor: National Science Foundation (IGERT Program on Integratively Engineered Biointerfaces at Rutgers); Grant number: DGE-0333196; Grant sponsor: NIH; Grant number: 2R25 GM58389; Grant sponsor: National Science Foundation; Grant numbers: IBN-0234206, IBN-0548543; Grant sponsor: March of Dimes Foundation; Grant number: 1-FY04-107; Grant sponsor: National Library of Medicine [by NIH Integrated Advanced Information Management Systems (IAIMS)]; Grant number: 2G08LM06230-03A1; Grant sponsor: Busch Biomedical, New Jersey Governor's Council on Autism Pilot.

REFERENCES

1. McAllister AK. Cellular and molecular mechanisms of dendrite growth. Cereb Cortex 2000;10:963–973. [PubMed: 11007547]
2. Firestein BL, Brenman JE, Aoki C, Sanchez-Perez AM, El-Husseini AE, Bredt DS. Cypin: a cytosolic regulator of PSD-95 postsynaptic targeting. Neuron 1999;24:659–672. [PubMed: 10595517]
3. Akum BF, Chen M, Gunderson SI, Riefler GM, Scerri-Hansen MM, Firestein BL. Cypin regulates dendrite patterning in hippocampal neurons by promoting microtubule assembly. Nat Neurosci 2004;7:145–152. [PubMed: 14730308]
4. Chen M, Lucas KG, Akum BF, Balasingam G, Stawicki TM, Provost JM, Riefler GM, Jornsten RJ, Firestein BL. A novel role for snapin in dendrite patterning: interaction with cypin. Mol Biol Cell 2005;16:5103–5114. [PubMed: 16120643]
5. Yuan G, Bin JC, McKay DJ, Snyder FF. Cloning and characterization of human guanine deaminase. Purification and partial amino acid sequence of the mouse protein. J Biol Chem 1999;274:8175–8180. [PubMed: 10075721]
6. Paletzki RF. Cloning and characterization of guanine deaminase from mouse and rat brain. Neuroscience 2002;109:15–26. [PubMed: 11784697]
7. Liaw SH, Chang YJ, Lai CT, Chang HC, Chang GG. Crystal structure of *Bacillus subtilis* guanine deaminase: the first domain-swapped structure in the cytidine deaminase superfamily. J Biol Chem 2004;279:35479–35485. [PubMed: 15180998]
8. Chang YJ, Huang CH, Hu CY, Liaw SH. Crystallization and preliminary crystallographic analysis of *Bacillus subtilis* guanine deaminase. Acta Crystallogr 2004;60(Pt 6):1152–1154.
9. Kumaran D, Burley SK, Swaminathan S. Crystal structure of guanine deaminase from C. acetobutylicum with bound guanine in the active site, to be published.
10. Vriend G. WHAT IF: a molecular modeling and drug design program. J Mol Graphics 1990;8:52–56.
11. Kneller DG, Cohen FE, Langridge R. Improvements in protein secondary structure prediction by an enhanced neural network. J Mol Biol 1990;214:171–182. [PubMed: 2370661]
12. Rost B, Sander C. Prediction of protein secondary structure at better than 70% accuracy. J Mol Biol 1993;232:584–599. [PubMed: 8345525]
13. Cuff JA, Clamp ME, Siddiqui AS, Finlay M, Barton GJ. JPred: a consensus secondary structure prediction server. Bioinformatics (Oxford, England) 1998;14:892–893.
14. Case DA, Cheathan TE, Darden T, Gohlke H, Luo R, Merz KM, Onufriev A, Simmerling C, Wang B, Woods RJ. The Amber biomolecular simulation programs. J Comput Chem 2005;26:1668–1688. [PubMed: 16200636]
15. Charych EI, Akum BF, Goldberg JS, Jornsten RJ, Rongo C, Zheng JQ, Firestein BL. Activity-independent regulation of dendrite patterning by postsynaptic density protein PSD-95. J Neurosci 2006;26:10164–10176. [PubMed: 17021172]
16. Castagnetto JM, Hennessy SW, Roberts VA, Getzoff ED, Tainer JA, Pique ME. MDB: the Metalloprotein Database and Browser at The Scripps Research Institute. Nucleic Acids Res 2002;30:379–382. [PubMed: 11752342]

17. Pettersen EF, Goddard TD, Huang CC, Couch GS, Greenblatt DM, Meng EC, Ferrin TE. UCSF Chimera—a visualization system for exploratory research and analysis. J Comput Chem 2004;25:1605–1612. [PubMed: 15264254]

18. Outten CE, O'Halloran TV. Femtomolar sensitivity of metalloregulatory proteins controlling zinc homeostasis. Science 2001;292:2488–2492. [PubMed: 11397910]

19. MacDonald RS, Wollard-Biddle LC, Browning JD, Thornton WH Jr, O'Dell BL. Zinc deprivation of murine 3T3 cells by use of diethylenetrinitrilopentaacetate impairs DNA synthesis upon stimulation with insulin-like growth factor-1 (IGF-1). J Nutr 1998;128:1600–1605. [PubMed: 9772124]

20. Paski SC, Xu Z. Labile intracellular zinc is associated with 3T3 cell growth. J Nutr Biochem 2001;12:655–661. [PubMed: 12031259]

21. Yamasaki S, Sakata-Sogawa K, Hasegawa A, Suzuki T, Kabu K, Sato E, Kurosaki T, Yamashita S, Tokunaga M, Nishida K, Hirano T. Zinc is a novel intracellular second messenger. J Cell Biol 2007;177:637–645. [PubMed: 17502426]

22. Deo RC, Schmidt EF, Elhabazi A, Togashi H, Burley SK, Strittmatter SM. Structural bases for CRMP function in plexin-dependent semaphorin3A signaling. EMBO J 2004;23:9–22. [PubMed: 14685275]

23. Accelrys, Inc.. InsightII. San Diego: Accelrys Inc; 2000.

24. Lopez, R.; Programme, S.; Loyd, A. ClustalW WWW service at the European Bioinformatics Institute. 2006. Available online at http://www.ebi.ac.uk/clustalw.

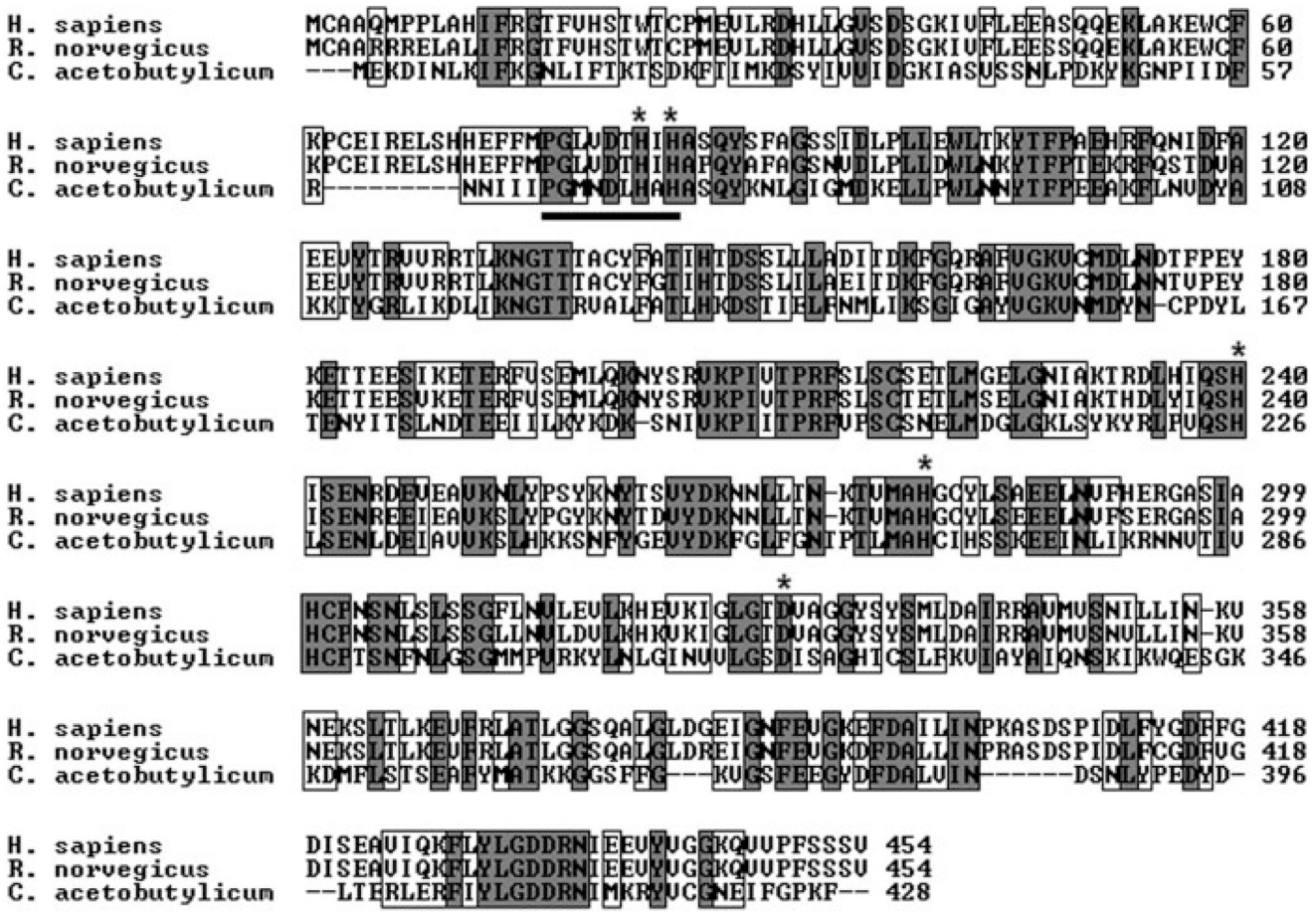

Figure 1.

Sequence alignment of guanine deaminases. Conserved residues are shaded and boxed, while class specific residues are boxed within the sequence alignment. The gaps are indicated with (–). The nine-residue motif thought to be responsible for the zinc ion binding is highlighted with a bar.

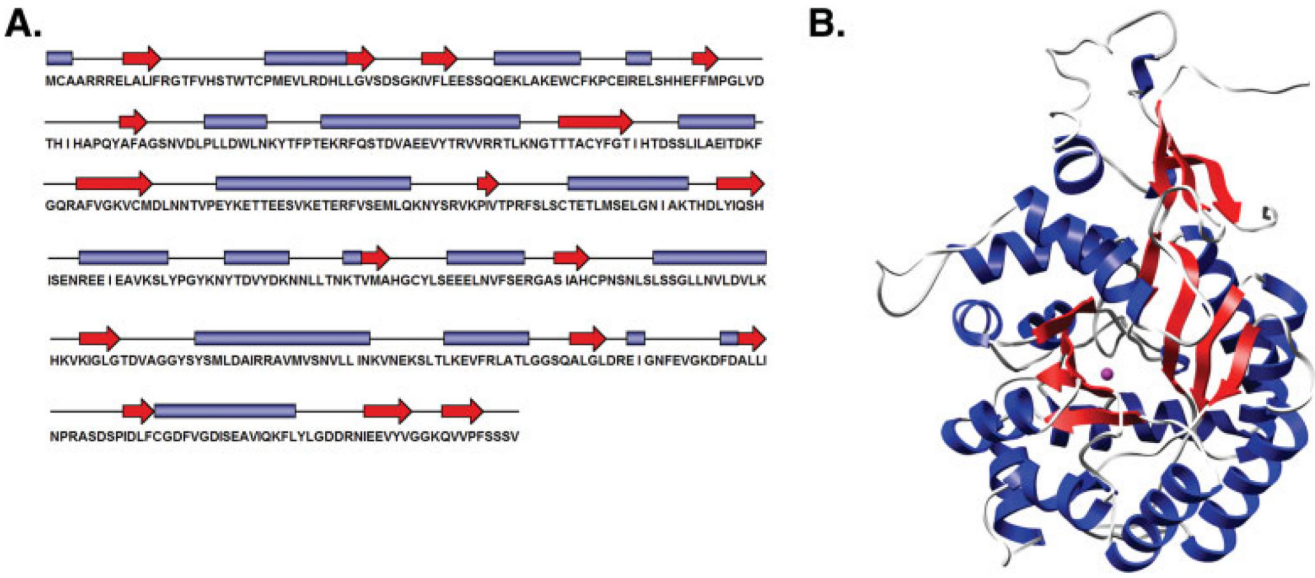

Figure 2.

Structural model of cypin by homology modeling. (**A**) Secondary structure prediction. The α-helices are represented as blue boxes and β-sheets as red arrows. (**B**) Homology model of rat cypin. The Zn^{2+} ion is colored magenta and the secondary structures colored as in (**A**). Molecular graphics images were produced using the UCSF Chimera package from the Resource for Biocomputing,[17] Visualization, and Informatics at the University of California, San Francisco (supported by NIH P41 RR-01081).

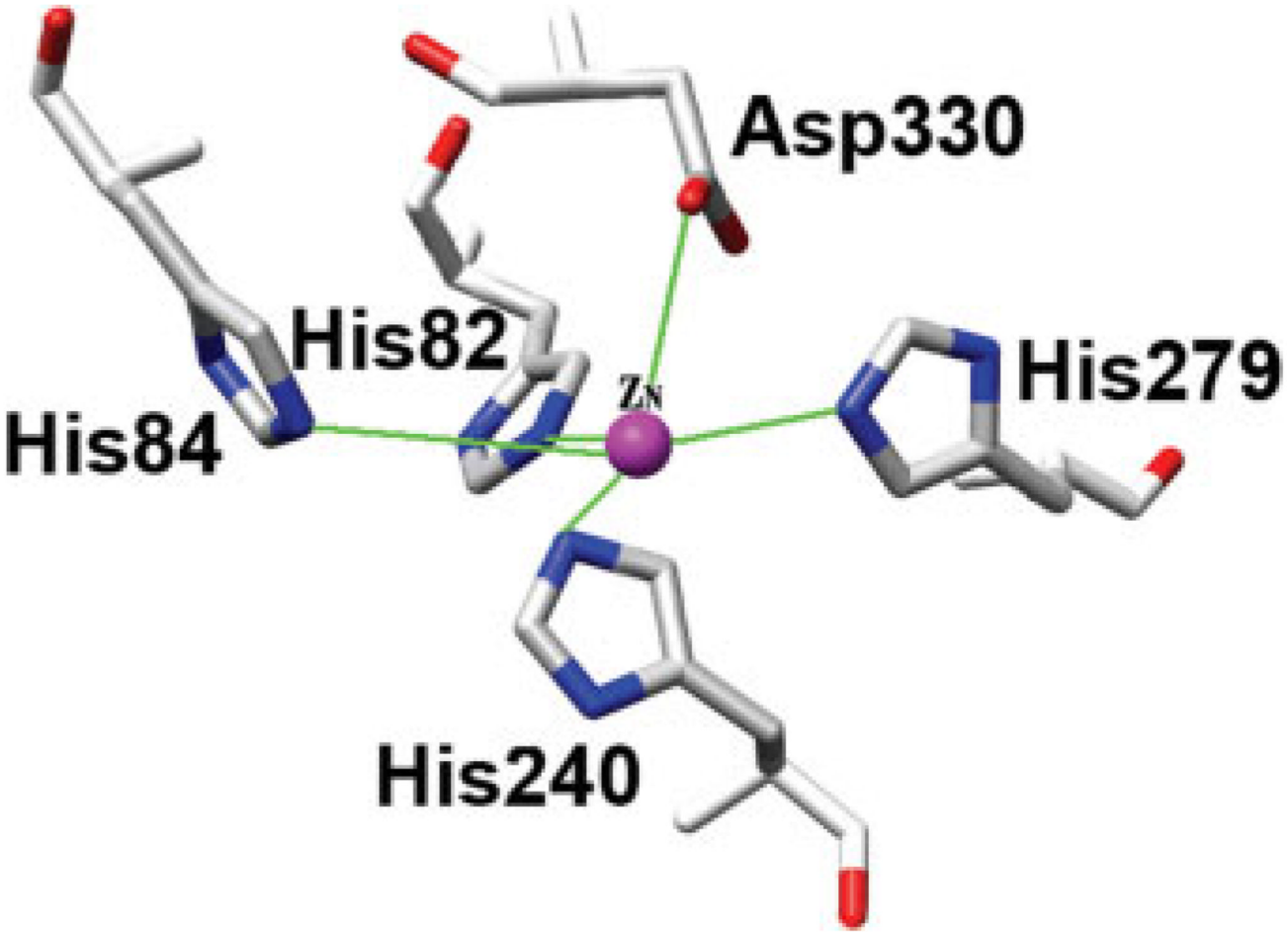

Figure 3.
Zn^{2+} scaffold coordination in cypin, the mammalian guanine deaminase. The protein residues are displayed as sticks and colored by atom-type (oxygen = red; nitrogen = blue). The Zn^{2+} ion is colored magenta. The ion coordination system is indicated by solid green lines.

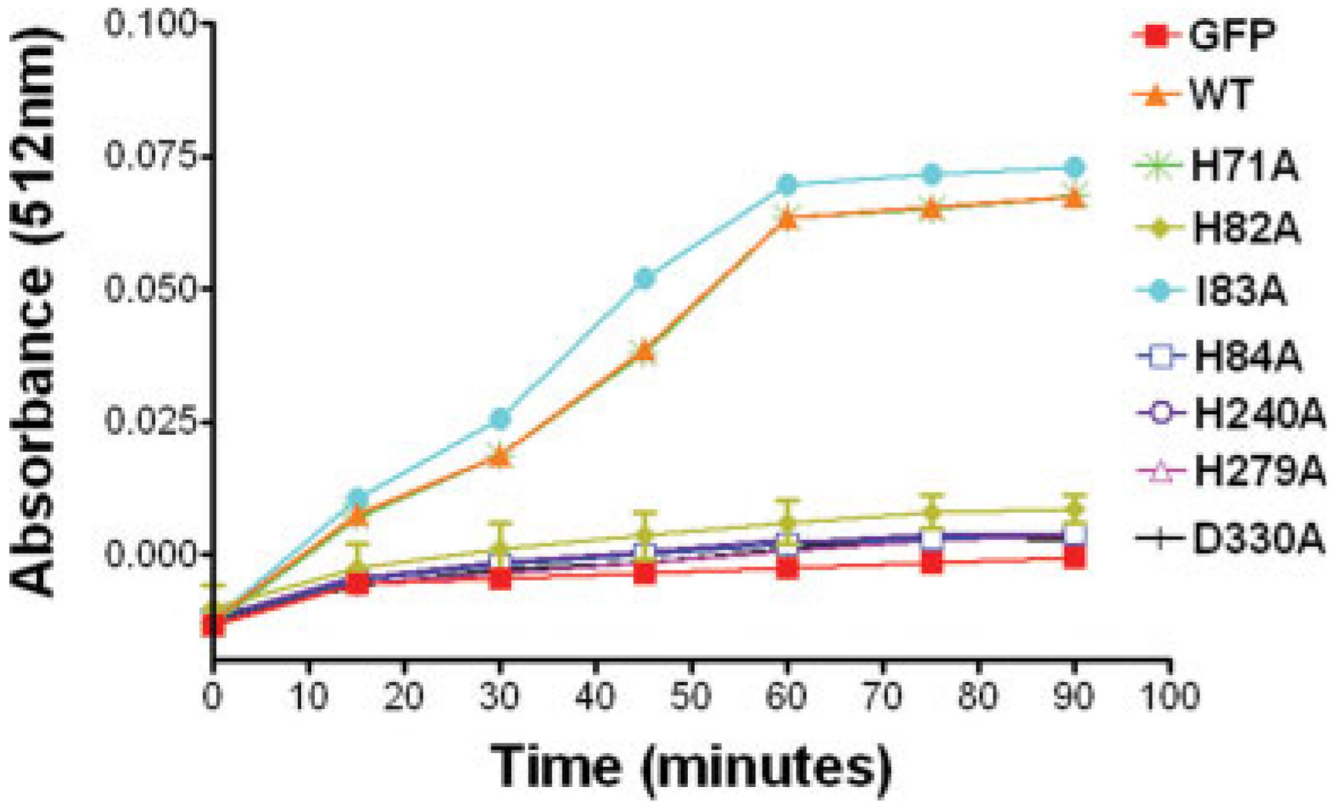

Figure 4.

Guanine deaminase activity is absent in cypin zinc-binding mutants. Lysates (50 μg) from COS-7 cells expressing GFP, GFP-cypin, GFP-cypin H71A, GFP-cypin H82A, GFP-cypin I83A, GFP-cypin H84A, GFP-cypin H240A, GFP-cypin H279A, and GFP-cypin D330A were examined using the Amplex Red dye in a colorimetric assay ($n = 3$). Cypin H71A and I83A were not predicted to be involved in zinc binding and were used as controls. $P < 0.01$ for wild type, H71A, and I83A cypin as determined by ANOVA followed by Dunnett's multiple comparisons test compared with GFP as control. SEM values are showed for each datapoint; note that some values are smaller than the data symbols.

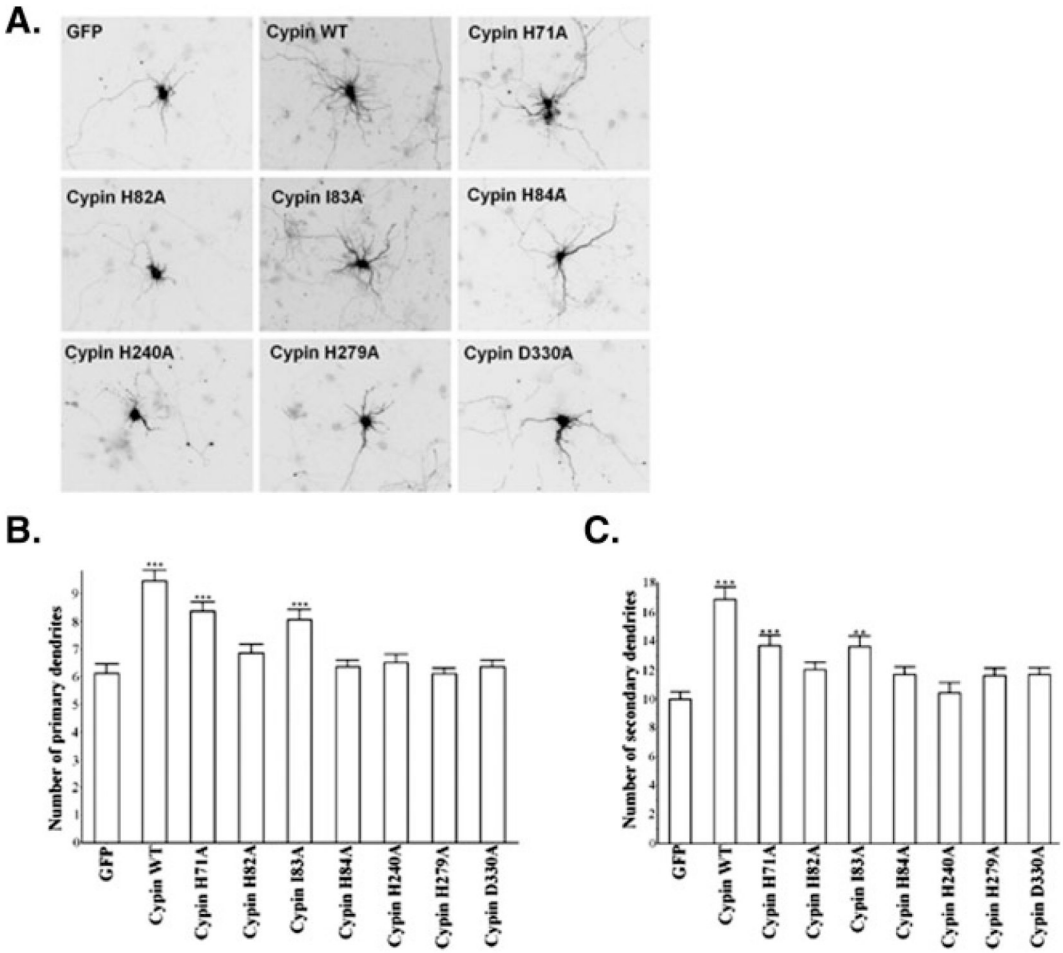

Figure 5.

Zinc-binding mutations eliminate cypin-promoted increases in dendrite number. (**A**) Immunostaining for GFP shows dendrite morphology changes in primary hippocampal neurons overexpressing GFP-cypin single substitution mutations. (**B**) Average number of primary dendrites in hippocampal neurons overexpressing GFP, GFP-cypin, GFP-cypin H71A, GFP-cypin H82A, GFP-cypin I83A, GFP-cypin H84A, GFP-cypin H240A, GFP-cypin H279A, or GFP-cypin D330A ($n = 35$). ***$P < 0.001$ and **$P < 0.01$ by ANOVA followed by Dunnett's multiple comparison test compared with GFP as control. (**C**) Average number of secondary dendrites as in (A).

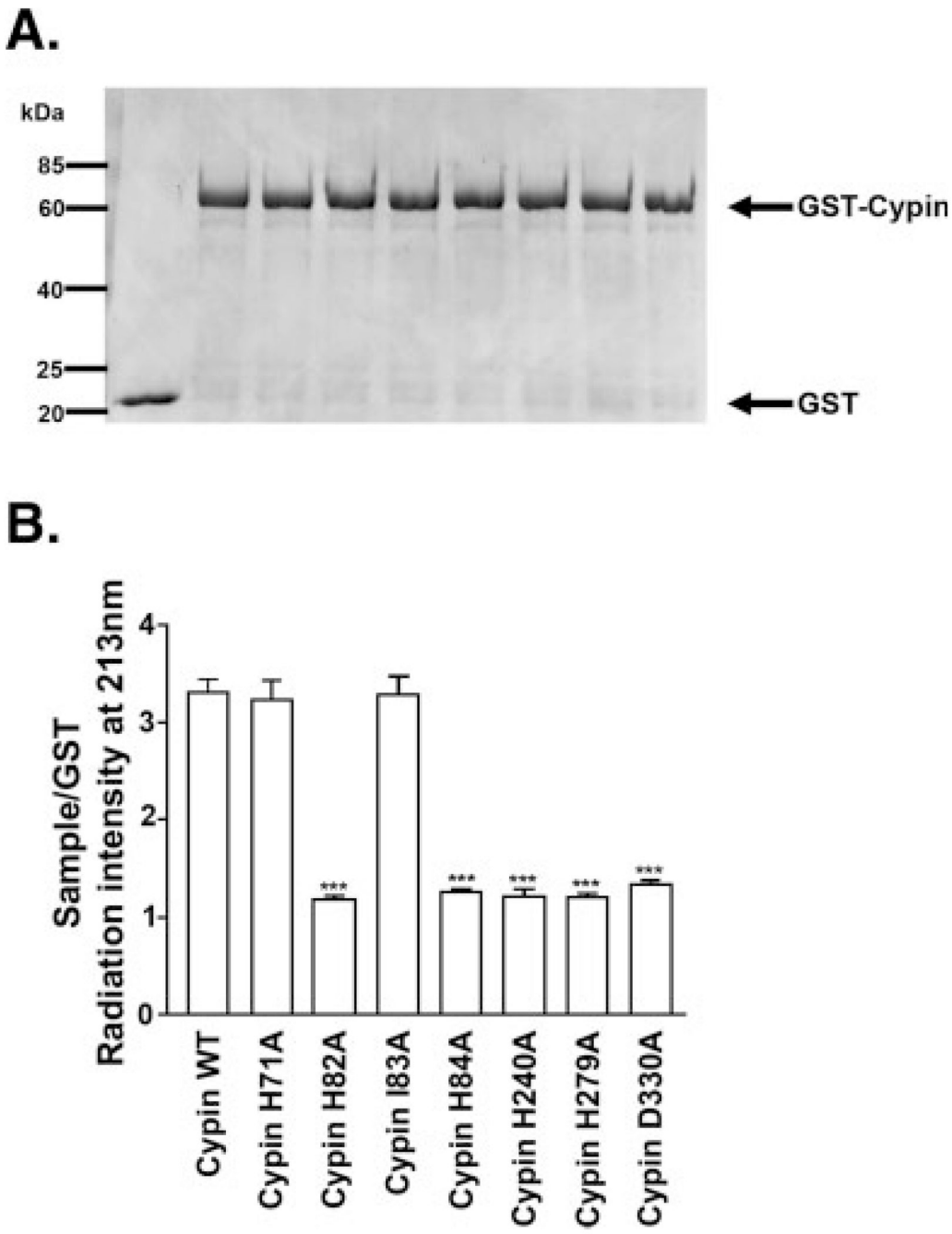

Figure 6.

ICP-OES demonstrates that His82, His84, His240, His279, and Asp330 are crucial residues for zinc-binding to cypin. (**A**) Coomassie Blue-stained 10% SDS-PAGE gel of 2 μg of each purified GST fusion protein. Traces of GST are present in GST-cypin and GST-cypin mutant preparations, due to a small amount of proteolysis often seen with our purification protocol. (**B**) Bar graph summarizing the average (n = 3) radiation intensity ratio for GST-cypin, GST-cypin H82A, GST-cypin H84A, GST-cypin H240A, GST-cypin H279A, and GST-cypin D330A detected at 213 nm. ***P < 0.001 by ANOVA followed by Student–Newman–Keuls multiple comparison test compared with GST as control.